Korean J. Chem. Eng., **25**(2), 191-198 (2008)

A numerical study on drying of porous media

Nima Amanifard and Akbar Khodaparast Haghi†

The University of Guilan, Faculty of Eng., P. O. Box 3756, Rasht, Iran
(*Received 13 March 2007 • accepted 5 July 2007*)

Abstract−In this study, two-dimensional conjugate heat and mass transfer in porous body and drying air during the drying process were numerically investigated by finite volume (FV) method, which guarantees the conservation of mass, momentum and the energy during the numerical solution. The full NS-equations (including buoyancy terms), energy equation and concentration equation are considered for external flow and for porous field coupled energy and moisture transfer equations are used. The numerically captured curve shows the same behavior of the drying process. Drying flow velocity shows proportional effect on moisture removal rate with a factor between $^1/_4$ and $^1/_5$ in Reynolds range of 50 to 1,000. Also, buoyancy forces have an effect on flow streamlines, the distribution of vapor concentration, moisture profile, and considerably increase drying rate. This increment was investigated in Reynolds number range of 50 to 1,000, and its minimum value was found in a Reynolds number of 1,000, which was about 15 percent.

Key words: Drying Process, Forced Convection, Mixed Convection, Numerical Study, Porous Media

INTRODUCTION

In capillary porous materials, moisture migrates through the body as a result of capillary forces and gradients of moisture content, temperature and pressure. This movement contributes to other heat transfer mechanisms while the eventual phase changes occurring within the material act as heat sources or sinks [1].

Drying is fundamentally a problem of simultaneous heat and mass transfer under transient conditions resulting in a system of coupled non-linear partial differential equations.

Luikov [2] and later Whitaker [3] defined a coupled system of partial differential equations for heat and mass transfer in porous bodies. Although they used different approaches to obtain equations, their formulations do not differ substantially from each other. Many numerical works have been executed in this field on basis of these two theories.

Kallel et al. [1] have developed a one-dimensional model for simultaneous heat and moisture transfer in porous materials. Also Ben Nasrallah and Perre [4]; and Murugesan et al. [5] have used one-dimensional models in studying heat and mass transfer during convective drying of porous media.

Ferguson and Lewis [6] studied the drying problem of timber with a two-dimensional model. Comini and Lewis [7] have used the finite element method for solution of two-dimensional heat and mass transfer in porous media.

All of the above listed studies have estimated heat and mass transfer between porous materials and drying fluid by coefficients obtained from standard correlations based on boundary layer equations, and more of them assumed an analogy between heat and mass transfer coefficients. However, since the actual process of drying is a conjugate problem, the heat and mass transfer to and from the porous solid have to be studied along with the flow field.

Dolinskey et al. [8] in a conjugate study of paper drying have shown that results of solution by conjugate view differ considerably from those of a decoupled system. Also, the analogy between heat and mass transfer coefficients may not exist in reality, even in drying of one-dimensional objects.

Masmoudi and Prat [9] found that the mentioned analogy holds true only for the initial period of unsaturated sand drying; and for the later part of drying, the heat and mass transfer coefficients at the interface may not satisfy the analogy, due to the non-uniformity of moisture and temperature distribution at the interface resulting from the conjugate nature of transfers.

Oliveira and Haghighi [10] have studied drying of wood as a conjugate problem. They have used boundary layer equations for flow field, and presented temperature and moisture contours during the process.

Murugesan et al. [11] have applied a two-dimensional model for brick drying. They used Navier-Stokes equations for flow field including buoyancy terms in their conjugate analysis. They concluded that restricting heat and mass transfer to the top surface of a two-dimensional porous body will cause considerable errors in the solution. They also have shown that neglecting buoyant forces in flow analysis leads to considerable differences in heat and mass transfer values and lower drying rate, in Reynolds number of 200.

Younsi et al. [12] studied conjugate heat and mass transfer during high-temperature heat treatment behavior numerically. They solved model equations by the commercial package FEMLAB for the temperature and moisture content. Comparison of their numerical and experimental results has shown good agreement.

In the majority of the previous conjugate studies, the buoyancy effects have been simply ignored in flow field analysis, except the study performed by Murugesan et al. [11]. The solution method used in [11] is a finite volume approach and is related to an unsteady problem. In this article we have tried to use a much more conservative method for calculation of energy and momentum fluxes. Regarding the weak capability of the finite element methods (specially in their flux averaging steps), the motivation of the current work concerns solving the same two-dimensional conjugate problem with a

†To whom correspondence should be addressed.
E-mail: Haghi@Guilan.ac.ir

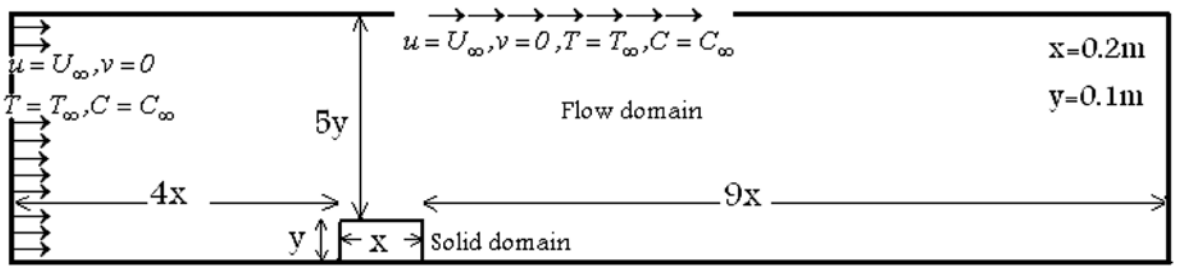

Fig. 1. Geometry of computational field.

finite volume approach which fundamentally guarantees the energy and the mass fluxes to be conserved during the solution and the discretization procedures. However, using the same mesh and consequently the same cells, the entire solution domain highlights the ability of the finite volume approach on using unstructured grids. On the other hand, the solution is extended to a higher Reynolds numbers (1,000) despite a Reynolds number of 200 reported by Murugensan et al. [11], to give a wider range study of the buoyancy effects not only on temperature and the moisture content, but also on flow patterns during the drying process.

MODELING

1. Problem Statement

The problem model, including corresponding boundary conditions, is shown in Fig. 1. The problem considers a sample of rectangular brick exposed to convective airflow. The brick is assumed to be saturated with water initially. The governing moisture removal from brick to air exceeds in the causing of concentration gradient between air in the vicinity of the body and free stream air. Flow is incompressible and thermophysical properties are taken to be constant. The initial moisture content of the brick is 0.13 kg/kg of dry solid, and the solid temperature is set to 293 K and the drying air has a 50% relative humidity. At Reynolds 200 the air velocity is 0.02 m/s. The thermal conductivity of the brick is 1.8 W/mK, and the thermal capacity is set to 1,200 J/kgK. The brick density is set to 1,800 kg/m^3.

Non-isothermal diffusion coefficient of porous body in vapor phase, $D_{tv}=1(10)^{-12}$

Non-isothermal diffusion coefficient of porous body in liquid phase, $D_{tl}=1(10)^{-12}$

Iso-thermal diffusion Coefficient of porous body in vapor phase, $D_{mv}=1(10)^{-12}$

Iso-thermal diffusion Coefficient of porous body in liquid phase, $D_{ml}=1(10)^{-8}$

Enthalpy of Evaporation (Initial value), $H_{fg}=2{,}454$ Kj/KgK

Mass diffusion coefficient of vapor in air, Diff$=0.256(10)^{-4}$

Fluid thermal conductivity, $K_f=0.02568$

Porous body thermal conductivity, $K_s=1.8$

Buoyancy coefficient of temperature, $\beta=3.4129(10)^{-3}$ 1/K

Buoyancy coefficient of Concentration, $\beta'=0.0173$

2. Governing Equations for Solid (Brick)

The equations for porous solid phase as obtained by Kallel et al. [1], on the basis of continuum approach, were applied for numerical solution:

Energy equation

$$c^*\frac{\partial T}{\partial t}=\left(\frac{k}{\rho_0}+h_{fg}D_{tv}\right)\left(\frac{\partial^2 T}{\partial x^2}+\frac{\partial^2 T}{\partial y^2}\right)+h_{fg}D_{mv}\left(\frac{\partial^2 M}{\partial x^2}+\frac{\partial^2 M}{\partial y^2}\right) \quad (1)$$

Where

$$c^*=c_0+m_l c_l+m_v c_v$$

Moisture conservation equation

$$\frac{\partial M}{\partial t}=(D_{tl}+D_{tv})\left(\frac{\partial^2 T}{\partial x^2}+\frac{\partial^2 T}{\partial y^2}\right)+(D_{ml}+D_{mv})\left(\frac{\partial^2 M}{\partial x^2}+\frac{\partial^2 M}{\partial y^2}\right) \quad (2)$$

3. Governing Equations for Flow Field

Continuity

$$\frac{\partial u}{\partial x}+\frac{\partial v}{\partial y}=0 \quad (3)$$

Momentum equation (2D Navier-Stokes)

$$\frac{\partial u}{\partial t}+u\frac{\partial u}{\partial x}+v\frac{\partial u}{\partial y}=-\frac{1}{\rho}\frac{\partial P}{\partial x}+\upsilon\left(\frac{\partial^2 u}{\partial x^2}+\frac{\partial^2 u}{\partial y^2}\right) \quad (4)$$

$$\frac{\partial v}{\partial t}+u\frac{\partial v}{\partial x}+v\frac{\partial v}{\partial y}=-\frac{1}{\rho}\frac{\partial P}{\partial y}+\upsilon\left(\frac{\partial^2 v}{\partial x^2}+\frac{\partial^2 v}{\partial y^2}\right)+g\beta(T-T_\infty)+g\beta'(C-C_\infty) \quad (5)$$

Energy equation

$$\frac{\partial T}{\partial t}+u\frac{\partial T}{\partial x}+v\frac{\partial T}{\partial y}=\alpha\left(\frac{\partial^2 T}{\partial x^2}+\frac{\partial^2 T}{\partial y^2}\right) \quad (6)$$

Vapor concentration equation

$$\frac{\partial C}{\partial t}+u\frac{\partial C}{\partial x}+v\frac{\partial C}{\partial y}=D\left(\frac{\partial^2 C}{\partial x^2}+\frac{\partial^2 C}{\partial y^2}\right) \quad (7)$$

4. Boundary and Initial Conditions

Initially, the porous material is assumed to be at uniform moisture content (saturation value), and temperature (equal to air temperature).

$$T(x, y, 0)=T_0;\ M(x, y, 0)=M_0$$

The boundary conditions at the interface of solid and fluid are [13,14]

No slip condition

$u=0;\ v=0$

Continuity of temperature

$T_f=T_s$

Continuity of concentration

$C=C(T, M)_s$

Heat balance

$$(k+\rho_0 h_{fg} D_{tv})\frac{\partial T}{\partial n}+\rho_0 h_{fg} D_{mv}+\frac{\partial M}{\partial n}=k_f\frac{\partial T_f}{\partial n}+h_{fg} D\frac{\partial C}{\partial n} \quad (8)$$

Species flux balance

$$\rho_0\left(D_{tv}\frac{\partial T}{\partial n}+D_{mv}\frac{\partial M}{\partial n}\right)=D\frac{\partial C}{\partial n} \quad (9)$$

Boundary conditions for flow field are

Inlet boundary condition

$u=U_\infty$, $v=0$, $T=T_\infty$, $C=C_\infty$

Far stream boundary condition (upper boundary)

$u=U_\infty$, $T=T_\infty$, $C=C_\infty$

Outflow boundary condition

$$\frac{\partial u}{\partial x}=0$$

Also bottom surface of solid is taken adiabatic.

GRID DEPENDENCY

A structured mesh was used for computational work. Mesh clustering around body is illustrated in Fig. 2.

To clarify effect of mesh refinement on numerical solution, three meshes with different precision were used in numerical analysis:

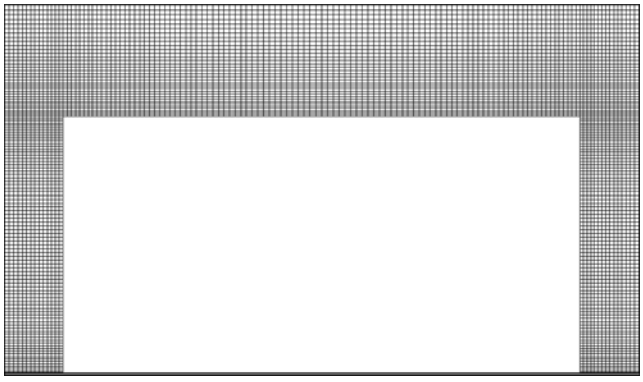

Fig. 2. Mesh structure over the porous material.

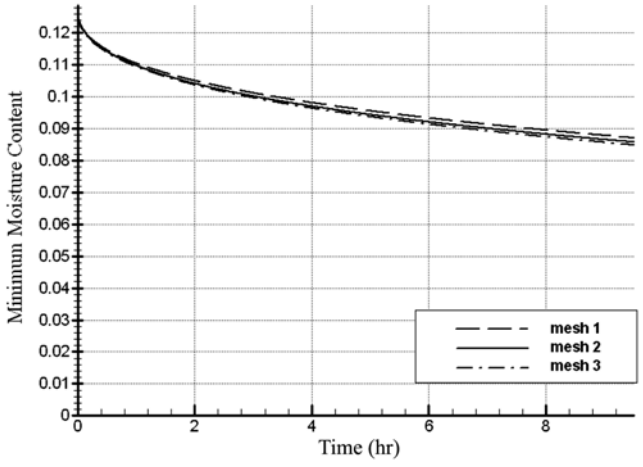

Fig. 3. Value of moisture content in leading edge obtained with three different meshes.

Mesh. 1, with 69120 total nodes.

Mesh. 2, with 108000 total nodes.

Mesh. 3, with 155520 total nodes.

As shown in Fig. 3, the value of moisture content in the leading edge (minimum value of moisture content) obtained by numerical solution with mesh 1 and mesh 2 in 9 hours has maximum difference of 1.28 percent, while for mesh 2 and mesh 3 the maximum difference is 0.66 percent. So mesh 2 seems to be optimum in accuracy and run-time, and therefore we decided to continue the computational work.

NUMERICAL SOLUTION

In each time-step, following items should be carried out:

1. Solution of two-dimensional flow field equations (continuity+ NS) by SIMPLE algorithm, with finite volume scheme.

2. Solution of energy equation for fluid by ADI technique with finite difference scheme. Neumann boundary condition was used for interface, which was obtained from last time-step derivative value of solid temperature in Eq. (8).

3. Then energy equation for porous field is solved by ADI technique with finite difference scheme. Boundary condition at interface is the known value of fluid temperature.

4. Determining concentration distribution for the flow field. The solution is similar to step 2, but the boundary condition is obtained from Eq. (9) by explicit moisture content derivative at the interface.

5. Calculation of moisture content distribution for porous body. The solution is similar to step 3, but the boundary value of the moisture is obtained by the known fluid concentration (from previous step) value at interface.

Because of using explicit values in the solution procedure, we have to do internal repetition in each time-step, until internal conversion is reached for all four variables. After that, solution for next timestep starts.

RESULTS AND DISCUSSION

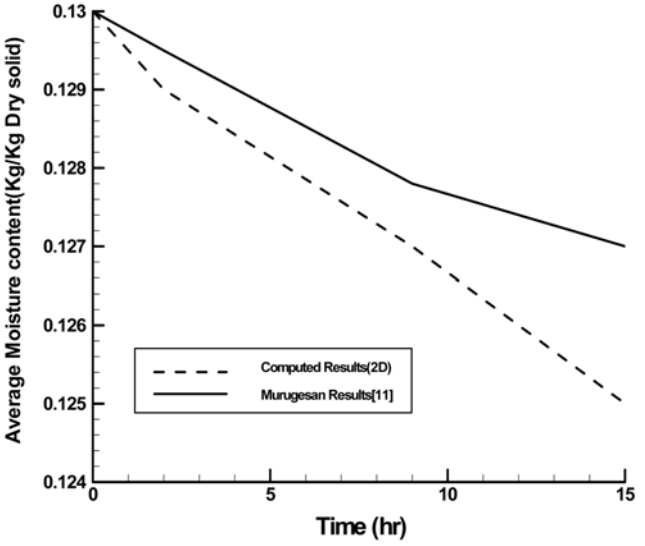

Fig. 4. Drying curve comparison of the present work, and the results of Murugesan et al. [11].

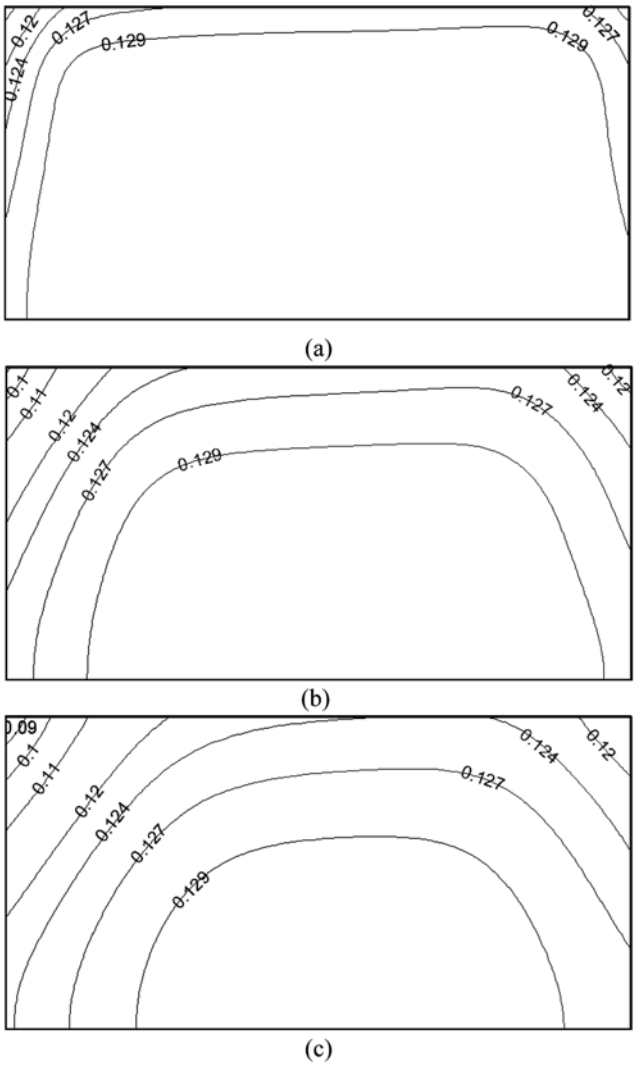

Fig. 5. Moisture content distributions (kg moisture/kg dry) during drying.
(a) t=2$^1/_2$ hr, (b) t=9 hr, (c) t=15$^1/_2$ hr

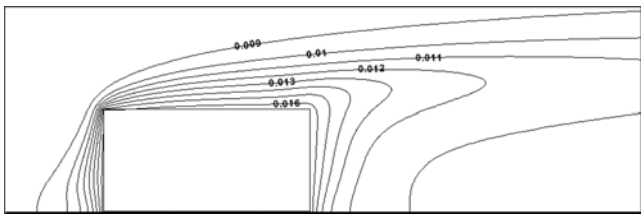

Fig. 6. Concentration contours in air around a porous body.

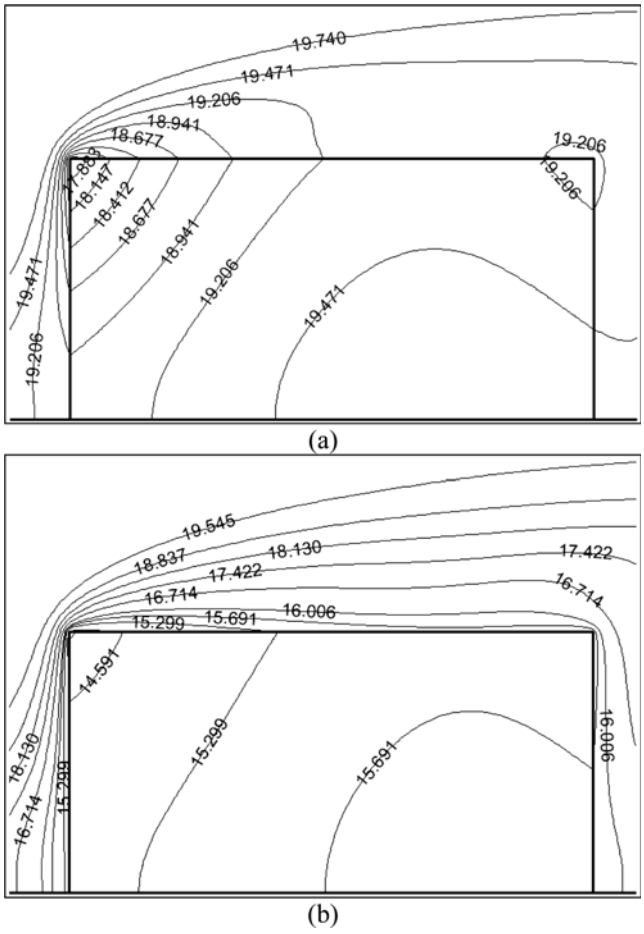

Fig. 7. Temperature distributions in porous body and around.
(a) t=2$^1/_2$ hr, (b) t=15$^1/_2$ hr

1. Validation and General Results

The drying curve of modeled brick in Re=200 is verified by results of Murugesan et al. [11]. As illustrated in Fig. 4, this comparison reveals that samples possessed almost nearly the same trend of moisture content reduction in the overall drying time of 15 hours. Nevertheless, the accuracy of above mentioned curves is within 0.6%.

The computational results of moisture content profile for Re=200 illustrates that drying rate in the region near the leading edge (which corresponds to maximum concentration gradient in adjacent air) is more than other regions in a porous body (Fig. 5). Gradually, drying spreads from that region to centric regions of the body.

Concentration values in air around a porous body are presented in Fig. 6. Concluding from this fig., the gradient of concentration in the body surface has shown a strong effect on moisture content distribution in body (as seen for the leading edge).

Temperature distributions in a porous body and around air in the course of drying are shown in Fig. 7. It's evident that the temperature value of the porous body near the leading edge decreases quickly as a result of higher moisture vaporization from the surface there, and this temperature drop is transferred to centric regions of the porous body.

2. Different Air Velocities

Numerical solution was executed for different velocities of drying fluid (different Reynolds number) to clarify the effect of this parameter. Fig. 8(a) to (c) shows streamlines around the body for Reynolds numbers of 50, 100 and 200. As shown in this fig, velocity increment in Re=50 to Re=100, results in more compactness of streamlines above the body, and then in Re=200 separation occurs, while a vortex forms on the upper surface.

In Fig. 9, contours of concentration around the body for denoted numbers of Reynolds are illustrated. It is obvious that a Reynolds increment results in a significant decrement in thickness of concentration boundary layer on the upper side (specially for leading edge)

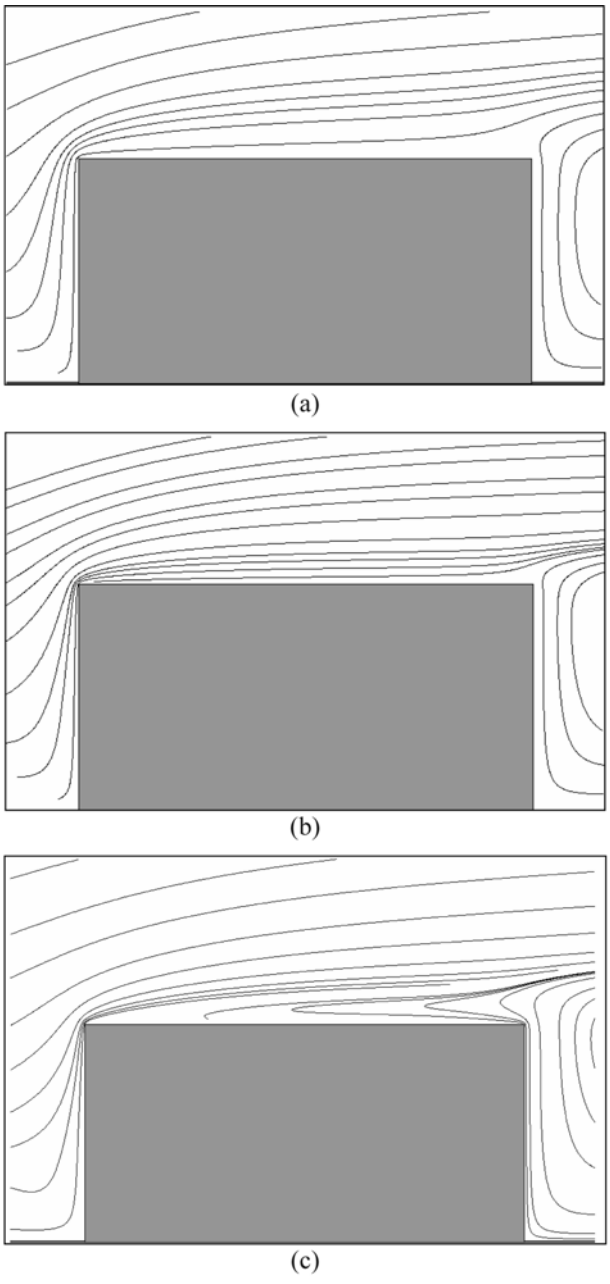

Fig. 8. Streamlines for different value of Re.
(a) Re_y=50, (b) Re_y=100, (c) Re_y=200

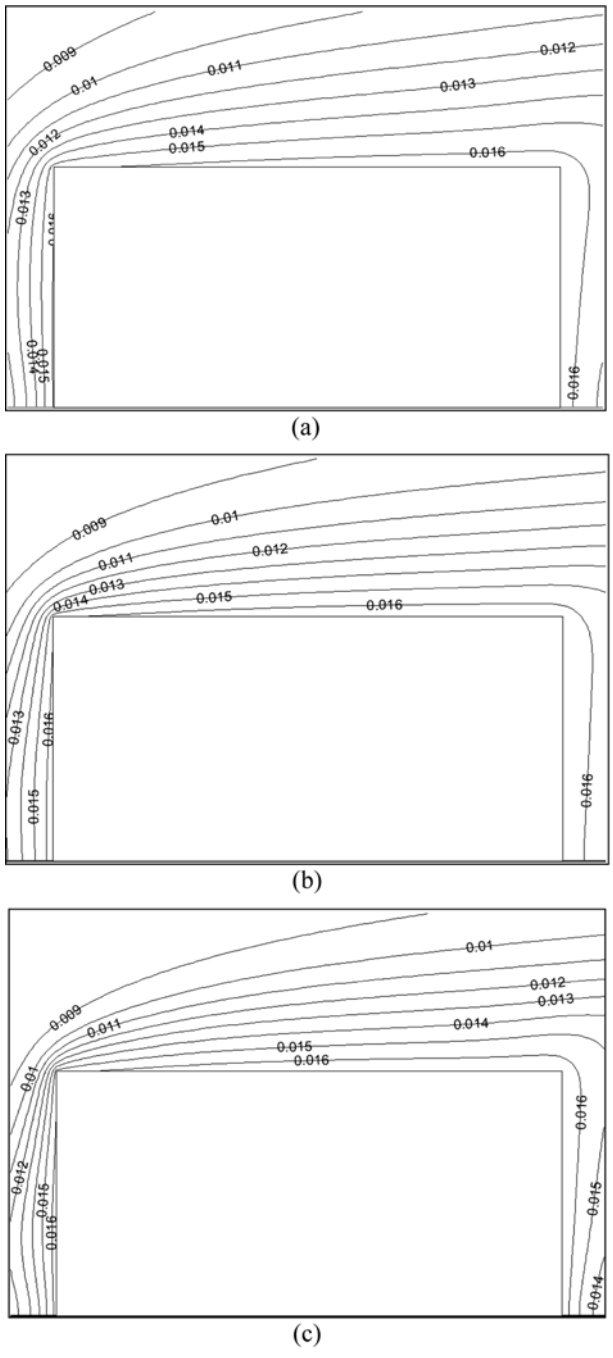

Fig. 9. Concentration contours for different value of Re.
(a) Re_y=50, (b) Re_y=100, (c) Re_y=200

due to changes in streamlines and velocity boundary layer.

For Re=100, moisture contents are less than those obtained for Re=50, especially for regions nearby the leading edge (Fig. 10(a) and (b)). This is mainly due to thinner concentration boundary layer aforementioned. In transition to Re=200 from Re=100 (Fig. 10(b) and (c)), this matter is satisfied just for the leading edge and left side of the body (as a result of vortex formation above the body in Re=200).

In Fig. 11 drying curves are shown for various Reynolds numbers ranging from 50 to 1,000. Effect of drying fluid velocity on process speed could be clearly analyzed. For example, the moisture removed after 5 hours of drying process for Re=100 is 15.4% more than corresponding value of Re=50. This difference is 17.5% for two Reynolds numbers of 500 and 200.

3. The Effect of Buoyancy

To study the contribution of buoyancy on flow patterns and consequently on the drying process, the computations were performed with and without buoyancy terms in flow equations (i.e., mixed and forced convection, respectively). Fig. 12 shows streamlines around the porous body in Re=200 for both the forced and mixed convection assumptions. As shown, buoyancy forces clustered the streamlines near vertical walls. In Fig. 13 the moisture content (MC) distribution is shown for $8^1/_4$ duration for both cases (Re=200). Obviously, the mixed convection results show a higher drying perfor-

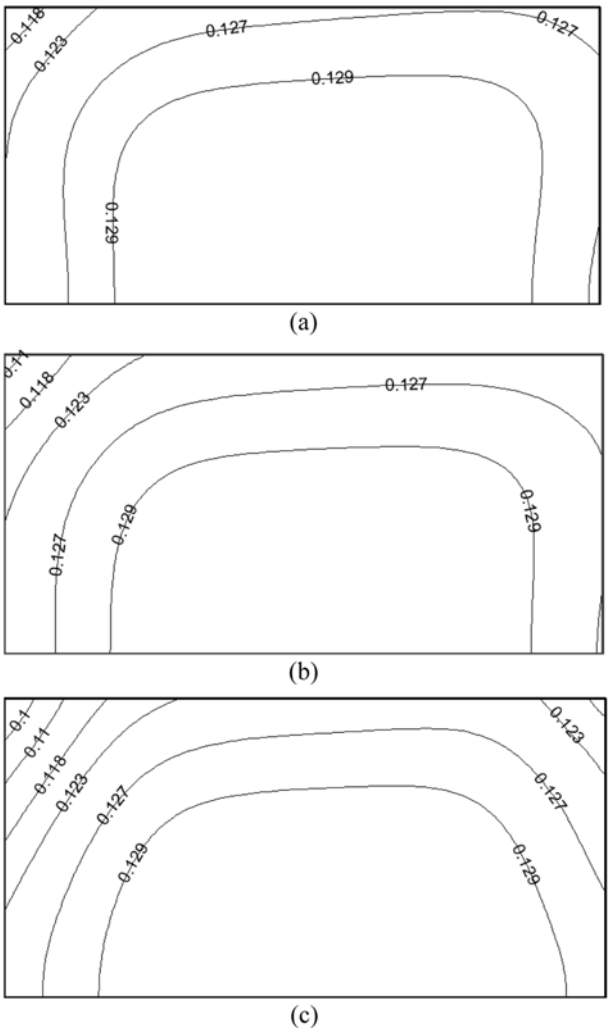

Fig. 10. Moisture content contours (kg moisture /kg dry) for different value of Re.
(a) Re_y=50, (b) Re_y=100, (c) Re_y=200

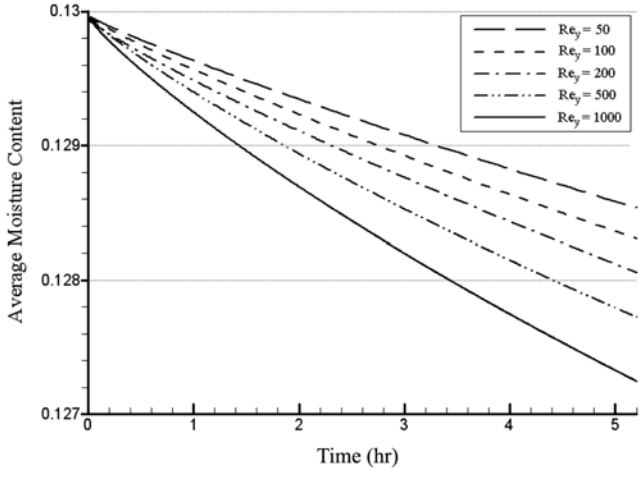

Fig. 11. Drying curves for Re=50 to 100.

mance.

A comparison between drying curves of mixed and forced as-

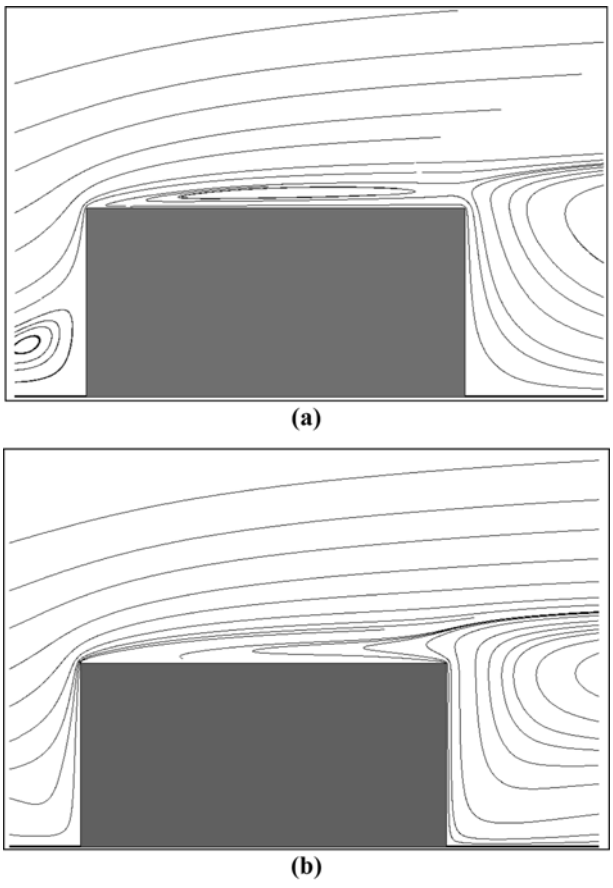

Fig. 12. Effect of buoyancy forces on streamlines in Re=200.
(a) forced convection (b) mixed convection

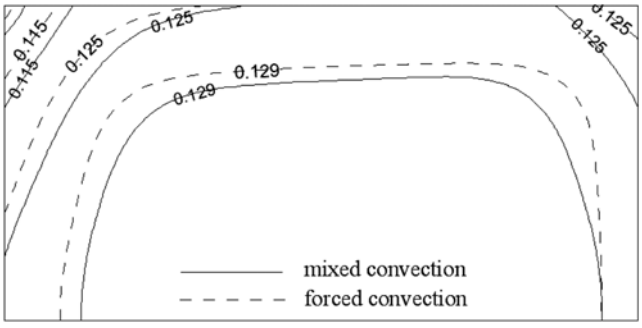

Fig. 13. Moisture profiles obtained by mixed and forced convection models in Re=200 (t=8$^{1}/_{4}$ hr).

sumptions is shown in Fig. 14. The decrease of (MC) has a lower rate in forced convection case for a 10 hour period, (e.g., 19.7 percent after 10 hours of drying). Consequently, the forced convection model underestimates drying rate noticeably in Re=200.

As stated above, the buoyancy force has a great contribution in drying prediction in Re=200. To investigate effect intensity in various drying fluid velocities (different Reynolds numbers), drying curves resulting by mixed and forced convection models in Reynolds numbers 50 and 1,000 (a practical range in drying) are illustrated in Fig. 15. Also, Fig. 16 shows average moisture fluxes (during initial 5 hours of process) obtained by each of the two models,

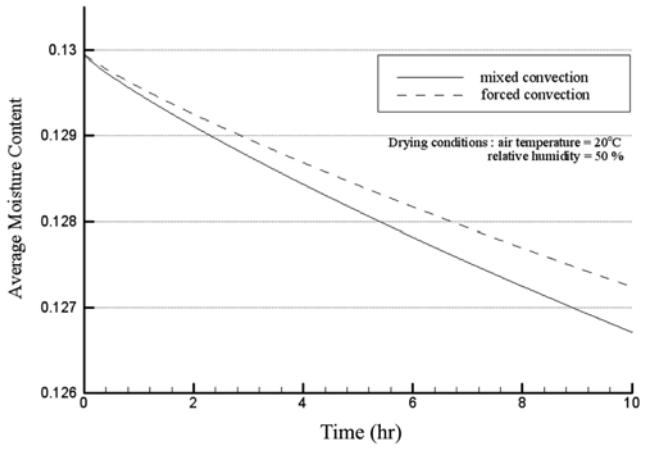

Fig. 14. Drying curve for mixed and forced convection models in Re=200.

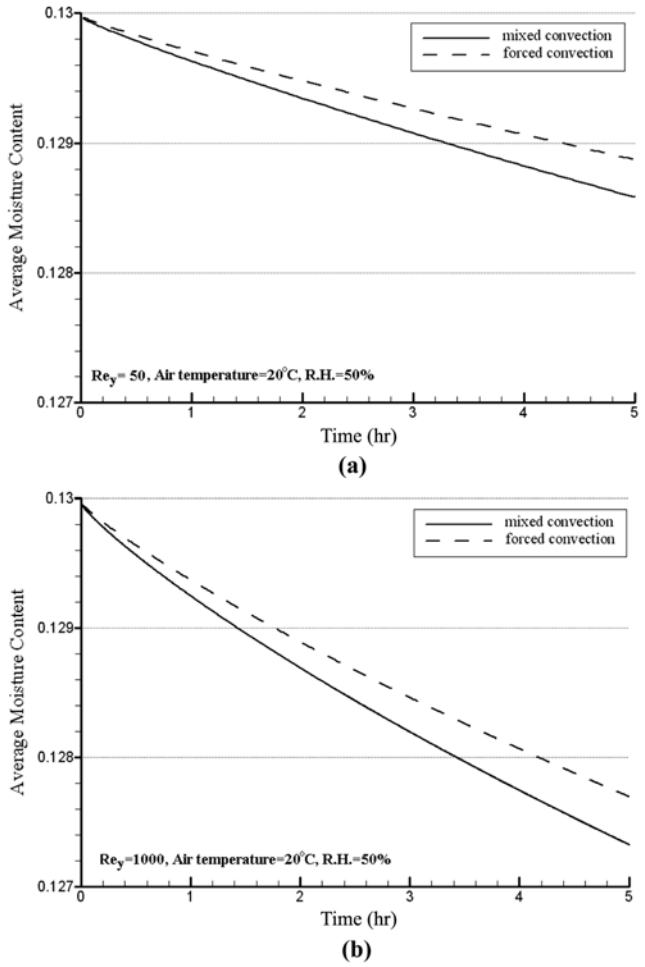

Fig. 15. Drying curve for mixed and forced convection models. (a) Re=50 (b) Re=1,000

and so in Table 1 the percentage increase in average moisture flux by taking buoyancy into account is listed for different Reynolds numbers. These figures and table imply that despite relative decreasing in drying rate with increasing Reynolds, the effect of buoyancy on the drying process in the whole Reynolds range of 50 to 1,000

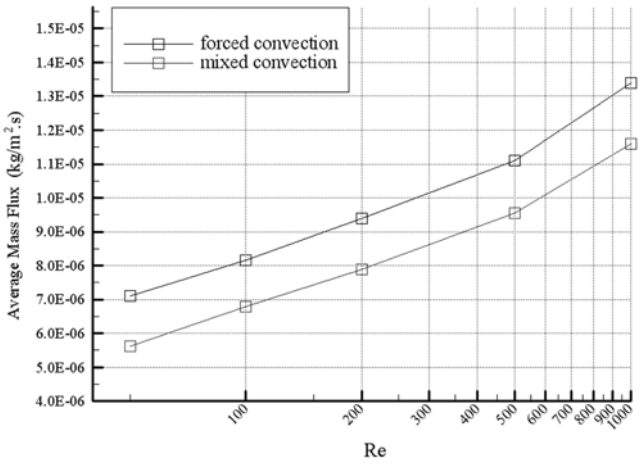

Fig. 16. Average mass flux during initial 5 hours of drying for mixed and forced convection models.

Table 1. Effect of buoyancy on average moisture flux for different Reynolds numbers

Re	Percentage increase in average moisture flux
50	26%
100	20%
200	19%
500	16%
1,000	15%

are considerable. So, in the denoted range of Re, which includes most practical velocities in porous bodies drying (especially clay products drying), ignoring buoyancy effects in flow analysis will impose noticeable error into computations. In other words, forced convection model has not enough accuracy for drying process analysis in the governing range.

CONCLUSION

Using an FV method, which in this article employed pressure-based conservative algorithms, we performed a two-dimensional conjugated solution that guarantees the conservation laws despite the finite element methods.

By studying the drying process in a variety of flow velocities (various Reynolds number), it is observed that airflow velocity increment has a proportional effect on drying rate, with a factor between $^1/_4$ and $^1/_5$.

Moisture profiles and drying rate are considerably affected by buoyancy forces. Moisture removal from a porous body surface for a mixed convection model is more than forced convection in of the entire Reynolds range of 50 to 1,000. So, it's suggested to take into consideration buoyancy effects in analysis of flow around porous bodies in drying or other similar processes.

NOMENCLATURE

β : coefficient of thermal expansion
c : specific heat

c^* : specific heat of porous medium
C : density of vapor
D_{ij} : diffusion coefficient of moisture
g : acceleration of gravity
h : vapor enthalpy per mass
h_{fg} : vapor enthalpy
h_m : mass transfer coefficient
k : thermal conductivity
m : mass
M : moisture per mass of porous medium
P : fluid pressure
ρ : density
t : time
T : temperature
T_∞ : ambient temperature
u : components of velocity in y direction
U_∞ : uniform velocity of fluid
v : components of velocity in x direction

REFERENCES

1. F. Kallel, N. Galanis, B. Perrin and R. Javelas, *J. Heat Transfer ASME Trans*., **115**, 724 (1993).
2. A. V. Luikov, *Heat and mass transfer in capillary-porous bodies*, Pergamon Press (1966).
3. S. Whitaker, *Advances in Heat Transfer*, **13**, 119 (1977).
4. S. Ben Nasrallah and P. Perre, *Int. J. Heat Mass Transfer*, **31**(5), 297 (1988).
5. K. Murugesan, K. N. Seetharamu and P. A. A. Narayana, *Heat and Mass Transfer*, **32**, 81 (1996).
6. W. J. Ferguson and R. W. Lewis, *A comparison of a fully non-linear and a partially non-linear heat and mass transfer of a timber drying problem*, Proceedings of 7th Conf. on Numerical methods in Thermal Problems, **VII**, Part 2, 973 (1991).
7. G. Comini and R. W. Lewis, *Int. J. Heat Mass Transfer*, **19**, 1387 (1976).
8. A. A. Dolinskey, A. S. Dorfman and B. V. Davidenko, *Int. J. Heat Mass Transfer*, **34**, 11, 2883 (1991).
9. P. Masmoudi and M. Prat, *Int. J. Heat Mass Transfer*, **34**(8), 1975 (1991).
10. L. S. Oliveira and K. Haghighi, *Numerical Heat Transfer*, **34**, 105 (1998).
11. K. Murugesan, H. N. Suresh, K. N. Seetharamu and P. A. A. Narayana, *J. Heat Mass Transfer*, **44**, 21, 4075 (2001).
12. R. Younsi, D. Kocaefe, S. Poncsak and Y. Kocaefe, *Appl. Therm. Eng.*, doi:10.1016 (2006).
13. H. N. Suresh, K. Murugesan, P. A. Narayana and K. N. Seetharamu, *Drying of porous material using finite element method*, 2nd Int. Conf. on CFD in minerals and process industries, Melbourne, Australia (1999).
14. Y. K. Yeo, K. S. Hwang, S. C. Yi and H. Kang, *Korean J. Chem. Eng.*, **21**, 761 (2004).